Improved Fabrication of Polymeric Optical Fiber Tweezers for Single Cell Detection

Sandra M. Rodrigues[1,2], Joana S. Paiva[1,2], Rita S. R. Ribeiro[2,3], Olivier Soppera[4], Pedro A. S. Jorge[1,2]

[1] *Physics and Astronomy Department, Faculty of Sciences, University of Porto, Portugal;* [2] *INESC Technology and Science, Portugal;* [3] *4Dcell and Elvesys, Paris, France.* [4] *Institute of Material Science of Mulhouse, France.*

pedro.jorge@inesctec.pt

Abstract: A new fabrication method of polymeric optical fiber tweezers with a multi-mode tip is presented. Preliminary results show higher robustness, improved ability for 2D trapping and differentiation of particles based on back-scattering analysis.

OCIS codes: 220.4000, 140.7010, 280.1350.

1. Introduction

Optical trapping (OT) was first reported by Arthur Ashkin in 1970 [1], where micron-sized particles were trapped in between two identical counter propagating laser beams. Since then optical trapping has evolved, and has been used in a variety of areas, with special emphasis in biology and biomedical applications [2, 3].

Most widely used and developed OT setups are nowadays based on bulk optics. Bulk OT present in some instances a series of limitations regarding manufacture costs, dimensions and portability. In this context, optical fiber tools can provide more versatile solutions towards the miniaturization of OT setups, given their small scale and ability to conduct light between the source and the target.

A diversity of fiber based OT has been reported, where different mechanisms were used to fabricate a lensed tip, including chemical etching, thermal pulling or high resolution micromachining using FIB [4] or fs laser systems [5]. In 2015, it was demonstrated, for the first time, 2D optical trapping of yeasts and synthetic particles [6], using a single mode fiber (SM) with a polymeric lens fabricated by a low cost self-guided photo-polymerization technique [10]. More recently these devices were used to simultaneously trap, detect and classify different micron-sized particles and cells through short-term back-scattered signal analysis [7, 8].

This work presents a novel tip configuration, where a multi-mode (MM) fiber segment is introduced at the tip of a SM fiber, enabling better control of the polymer lens features. The optimization of the fabrication process is addressed and a comparison study is conducted to understand how the new hybrid lenses perform against SM [8].

2. Methods

2.1. Fabrication Method

The fabrication of the fiber tip polymeric lenses (SM and SM+MM) is based on the photo-polymerization process described in references [6–10]. Several optical fiber tips were fabricated using the conventional fabrication method (SM) and the variant proposed here (SM+MM). In both instances, the photo-polymerization is initiated by a photo-chemical process induced by the energy of a radiation source of a wavelength matching the photo-initiator sensitivity. The free-radicals are created from excited states by the photo-initiator and they react with a monomer molecule to form the polymer. The monomer used was the pentaerythritol triacrylate (PETIA), and the photo-initiator was the Irgacur 819, whose working wavelength range goes from the 375 nm to 450 nm. The radiation source was a 405 nm diode laser (LuxX cw, 60 mW, Omicron).

In the fabrication of the new SM+MM tip, we start by cleaving the two types of optical fiber. A SM fiber at 980 nm (Thorlabs SM 980-5.8-125), the same used for the standard SM tips [6–9], and a section of a MM fiber (Thorlabs MM 0.22 NA, ϕ 50 μm, 250-1200 nm). The two fiber sections are then spliced together. Afterwards, the fiber is cleaved once again, near the splice region, leaving just a few micrometers of the MM section at the tip. Once the process is completed, the polymer tips are fabricated as previously described [6, 9]. The fiber is placed on a moving stage and dipped into the solution with the photo-initiator and monomer. A drop of liquid is then formed on its tip, which is exposed to the laser source, originating the polymer tip. Since the SM 980 fiber behaves as MM at 405 nm, care has to be taken to excite a fundamental mode. For this work, the LP_{02} mode was used.

Several different tips were fabricated for three different polymerization laser powers: 5 μW, 10 μW and 20 μW (measured at the fiber output, before polymerization). A solution containing a concentration of photo-initiator of 0.2% and a laser exposure time of 10 seconds were used in all cases.

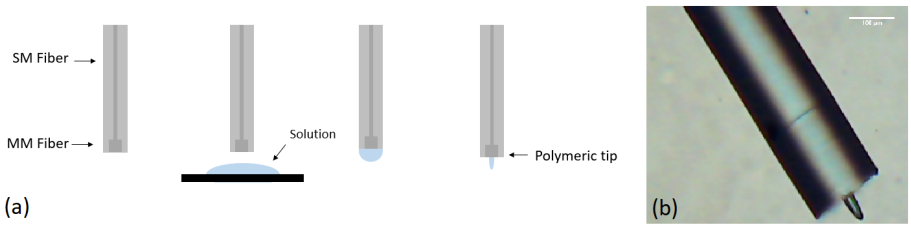

Fig. 1. (a) Fabrication steps of the micro-structures at the end of the fiber. (b) Polymeric lensed tip at the end of the fiber - a reflection from the splice site is visible, allowing to clearly distinguish the two different fibers.

2.2. *Setup for Optical Trapping and Back-Scattered Signal Acquisition*

The experimental setup used to trap and manipulate the particles consists of an inverted homemade microscope with a 20x objective, where a CMOS camera is used to acquire images of the trapping. The fiber that contains the micro-lens is controlled using a motorized micro-manipulator capable of handling the optical fiber in the x, y and z direction, and varying the inclination angle. Trapping can only occur at tilt angles above 30°, therefore the capillary holding the fiber was tilted to approximately 55°, to ensure stable trapping [9].

The lensed fiber was connected through the exit port of a 1x2 (50:50) optical coupler to a pigtail 980 nm laser diode (500 mW, Lumics) and the signal acquisition module. The latter included a photodetector to collect the back-scattered signal, and a data acquisition board (DAQ) from National Instruments for signal processing. A computer controlled both the DAQ and the laser enabling control of its input and output parameters.The output laser power was set to $\approx$ 15 mW at 980 nm during the trapping experiments, to avoid damaging the biological cells (yeast cells) while ensuring a stable trapping.

2.3. *Processing the Back-Scattered Signal*

Table 1. Table summarizing the back-scattered signal parameters that contributed to LDA (based on [6]).

Type	Group	Number	Feature/Parameter
Time Domain	Time Domain Statistics	1	Mean (M)
		2	Standard Deviation (SD)
		3	Skewness (Skew)
		4	Kurtosis (Kurt)
		5	Interquartile Range (IQR)
		6	Entropy (E)
	Time Domain Histogram	7	$\mu_{Nakagami}$
Frequency Domain	Discrete Cosine Transform (DCT)	8 ... 27	1st ... 20th Coefficient ($E_{DCT}[l^1]$...$E_{DCT}[l^{20}]$)
		28	Number of coefficients that capture 98% of the original signal (N_{DCT})
		29	Total spectrum Area Under Curve (AUC) (AUC_{DCT})
		30	Maximum peak amplitude ($Peak_{DCT}$)
		31	Total spectral power (P_{DCT})
	Wavelet Packet Decomposition	32 ... 37	Haar Relative Power 1st ... 6th level (E^1_{Haar} ... E^6_{Haar})
		38 ... 43	Db10 Relative Power 1st ... 6th level (E^1_{Db10} ... E^6_{Db10})

Two solutions were prepared with deionized water: one containing yeast cells (6-7 μm in diameter) and the other PMMA microspheres (8 μm of diameter). Once a polymeric tip was immersed in one of the solutions, two MATLAB scripts were used: one to modulate the laser signal using a 1 kHz frequency sinusoidal signal; and a second one, executed only after each particle was trapped, to acquire the back-scattered signal during 60 seconds at a sampling rate of 100 kHz. Signals were collected for 5 different particles for each class (Class 1 - PMMA particles and Class 2 - yeast cells). After acquisition, each signal was processed using a custom built MATLAB script [8]. First, the signal was downsampled to 5 kHz to reduce computational cost, and then filtered using a 500 Hz second order Butterworth high-pass filter, to remove low frequency noise. Then, each 60 s signal was split into 2 s portions, from which outliers (values corresponding to $\|$ z-score $\|$ >10) were removed. In a previous work [8], a set of 43 back-scattered signal derived parameters were used to successfully differentiate biological and synthetic particles. Those same parameters were extracted in this study from the signal portions and processed using the Linear Discriminant Analysis (LDA) method (please consult table 1 for a detailed description of the parameters). This method is able to generate a single parameter that results from a linear combination of a set of original features, in a way that better separates data classes. Afterwards, a statistical analysis was performed to evaluate the differentiation power of the final LDA-derived parameter, which allowed us to compare the sensing ability of the different polymeric tips. Since this feature was normally distributed, according to the Shapiro-Wilk Normality Test, the Student t-test was applied.

3. Results and Discussion

3.1. Characterization of Polymeric Tips

A study of the tip diameter variation was made as a function of the MM segment length (from 20 μm to 180 μm). This was repeated for three different fabrication optical power values - 5 μW, 10 μW and 20 μW. All other parameters were maintained: concentration of photo-initiator in the solution of $\approx$ 0.2%, exposure time of $\approx$ 10 seconds and excitation of LP_{02} mode.

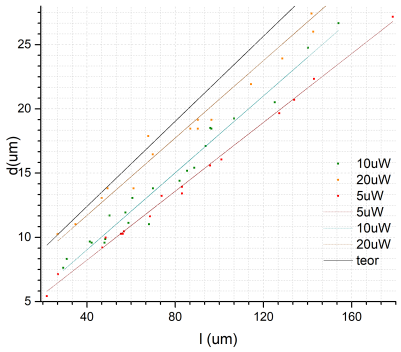

Fig. 2. Diameter of the output tip for different lengths of the MM section and three different polymerization power.

Assuming a diffraction limited laser beam, and the different core dimensions of the optical fibers, an expansion of the optical beam when passing from the SM fiber to the MM segment is expected, which can be calculated through the numerical aperture of the optical fiber (1), allowing to predict how much it will spread given a certain length l, and thus determine the diameter of the laser spot at the tip output (2).

$$N.A. = n_1 \sin\theta_m = \sqrt{n_{co}^2 - n_{cl}^2} \tag{1}$$

$$d_s = 2l \sin\theta + 5.8 \tag{2}$$

where n_1, n_{co} and n_{cl} are the refractive indexes of SM fiber core, MM fiber core and MM fiber cladding, respectively; l is the length of the MM section, and 5.8 is the SM fiber core radius. The light spot diameter at the fiber output will consequently determine the dimension of the micro-structure base, enabling to control its thickness and robustness.

The results presented in fig. 5 show that experimental values converge to the theoretical curve as the power increases. With increasing power an increase in the slope of the experimental fit was also verified, in a way that it approaches the theoretical expected value of 0.16. The same behavior is obtained for the value the function takes at $l = 0$. Considering this characteristic behavior, the tips obtained through the new method were categorized into two different types. Type A: lenses with base diameters lower than 15μm; and type B: lenses with base diameters higher than 15 μm (see fig. 3). Both types A and B lenses belong to the set of lens produced with 5 mW. We observed a variation of their radius as a geometrical consequence of the base diameter difference. A microscopic image of the polymeric fiber tip fabricated using standard SM fiber was named Type C and is also provided in fig 3.

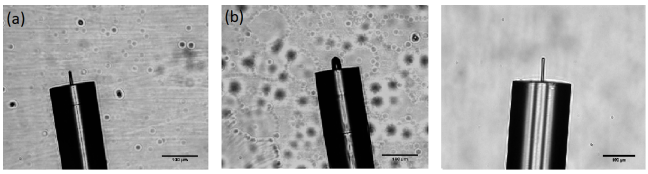

Fig. 3. (a) Type A lens with diameter of 10.27 μm and radius of 5.80 μm; (b) Type B lens with diameter of 27.16 μm and radius of 23.21 μm; (c) Type C lens with diameter of 5.61 μm and radius of 8.26 μm.

3.2. Back-Scattered Signal Analysis

The particles differentiation ability considering the back-scattered signal acquired using the three types of polymeric tips (A, B and C) was evaluated. All the three types could differentiate yeasts from PMMA particles with statistical

significance (at a level of 0.05), through signal portions of 2s. In fig. 4 we present the results obtained from the Student t-test. Considering that the differentiation power between classes is negatively correlated with the p-value resultant from the statistical analysis, we can conclude that the strongest differentiation ability is associated with the lens of type A. Thus, the variant of the fabrication method has indeed introduced an improvement on particles detection ability, since the p-value of the statistical comparison associated to the conventional single mode polymeric tip (type C) is the highest.

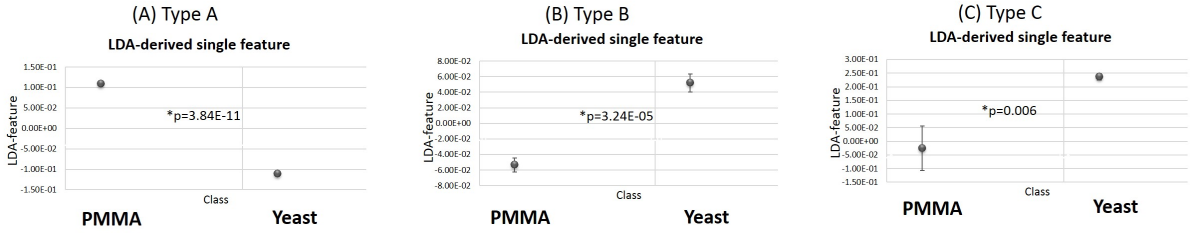

Fig. 4. Mean values across particles for the final LDA-derived feature for each class, considering the polymeric tip from (A) type A; (B) type B and (C) type C; and corresponding p-values obtained from the statistical test. Error bars represent standard errors. * - statistical significance at a level of 0.05.

This improvement is most likely due to the change in the numerical aperture of the lensed micro-structures. As they present a larger diameter compared to those produced by the conventional method, they have a larger numerical aperture, and thus, a better ability to collect the back-scattered radiation. However, if the aperture becomes too large, the lensed tip will also collect back-scattered radiation from areas where no particle is present. Hence the better results obtained by type A. On the other hand, an improvement of the trapping forces was also verified. Trapping forces with type A lens were measured to be twice the value of a conventional lens [9], while for type B, were $\approx$ 20 times larger.

4. Conclusions

In conclusion, we proposed here a variant of polymeric tips fabrication method on the top of optical fibers, based on the introduction of MM segment on the SM fiber. The lenses fabricated by this method presented slight changes in geometry in relation to those obtained by the conventional one regarding their diameter and curvature. Controlling these characteristics we attained a lens which has improved the ability to sense the class of trapped particles, in comparison with the conventional photo-polymerization fabrication method previously proposed.

5. Acknowledgments

This work was partly developed under the project NanoSTIMA, funded by the North Portugal Regional Operational Program (NORTE 2020), under the PORTUGAL 2020 Partnership Agreement, and through the European Regional Development Fund (ERDF). It was also funded by the Portuguese Foundation for Science and Technology (FCT) within the Grant PD/BD/135023/2017.

References

[1] Ashkin, A. Accelaration and trapping of particles by radiation pressure. *Phys. Rev. Lett.* **1970**, *24*, 156-159.

[2] Ashkin, A.; Dziedzic, J. M. Optical trapping and manipulation of viruses and bacteria. *Science* **1987**, *225*, 1517-1520.

[3] Zhong, Min-Chen et. al. Trapping red blood cells in living animals using optical tweezers. *NComms* **2013**, *4:1768*

[4] S. Cabrini; C. Liberale; D. Cojoc; A. Carpentiero; M. Prasciolu; S. Mora; V. Degiorgio; F. De Angelis; E. Di Fabrizio; Axicon lens on optical fiber forming optical tweezers, made by focused ion beam milling *Microelectron. Eng.* **2006**, *vol. 83* .

[5] S. R. Ribeiro, R.; Soppera, O.; G. Oliva, A.; Guerreiro, A.;S. Jorge, P. A.; New Trends on Optical fiber Tweezers. *Journal of Lightwave Technology* **2015**, *vol. 33, no. 16* .

[6] Ribeiro, R.S.R. et.al; Optical Fiber Tweezers Fabricated by Guided Wave Photo-Polymerization. *Photonics* **2015**, *2*,634-645.

[7] Rodrigues Ribeiro, Rita S.; Dahal, P.; Guerreiro, A.; Jorge, P.; Viegas, J.; Fabrication of Fresnel plates on optical fibers by FIB milling for optical trapping, manipulation and detection of single cells *Scientific Reports* **2017**, *7*.

[8] Paiva, J.S.; Ribeiro, R.S.R.; Cunha, J.P.S.; Rosa, C.C.; Jorge, P.A.S; Single Particle Differentiation through 2D Optical Fiber Trapping ans Back-Scattered Signal Statistical Analysis: an Exploratory Approach *Sensors* **2018**, *18*, 710.

[9] R. Ribeiro. Optical Fiber tools for single cell trapping and manipulation *Doctoral Thesis- University of Porto* **2017**.

[10] Soppera, O.; R. Jradi, S.; Lougnot, J.; Photopolymerization with microscale resolution: Influence of the phsysico-chemical and photonic parameters *Journal of Polymer Science Part A: Polymer Chemistry* **2008**, *46*.